MNRAS **460,** 3529–3544 (2016)
Advance Access publication 2016 May 20

doi:10.1093/mnras/stw1214

Luminosity distributions of Type Ia supernovae

C. Ashall,[1]★ P. Mazzali,[1,2] M. Sasdelli[1,2] and S. J. Prentice[1]

[1]*Astrophysics Research Institute, Liverpool John Moores University, IC2, Liverpool Science Park, 146 Brownlow Hill, Liverpool L3 5RF, UK*
[2]*Max-Planck-Institut für Astrophysik, Karl-Schwarzschild-Str. 1, D-85748 Garching, Germany*

Accepted 2016 May 18. Received 2016 May 18; in original form 2016 February 10

ABSTRACT

We have assembled a data set of 165 low redshift, $z < 0.06$, publicly available Type Ia supernovae (SNe Ia). We produce maximum light magnitude (M_B and M_V) distributions of SNe Ia to explore the diversity of parameter space that they can fill. Before correction for host galaxy extinction we find that the mean M_B and M_V of SNe Ia are -18.58 ± 0.07 and -18.72 ± 0.05 mag, respectively. Host galaxy extinction is corrected using a new method based on the SN spectrum. After correction, the mean values of M_B and M_V of SNe Ia are -19.10 ± 0.06 and -19.10 ± 0.05 mag, respectively. After correction for host galaxy extinction, 'normal' SNe Ia ($\Delta m_{15}(B) < 1.6$ mag) fill a larger parameter space in the width–luminosity relation than previously suggested, and there is evidence for luminous SNe Ia with large $\Delta m_{15}(B)$. We find a bimodal distribution in $\Delta m_{15}(B)$, with a pronounced lack of transitional events at $\Delta m_{15}(B) = 1.6$ mag. We confirm that faster, low-luminosity SNe tend to come from passive galaxies. Dividing the sample by host galaxy type, SNe Ia from star-forming (S-F) galaxies have a mean $M_B = -19.20 \pm 0.05$ mag, while SNe Ia from passive galaxies have a mean $M_B = -18.57 \pm 0.24$ mag. Even excluding fast declining SNe, 'normal' ($M_B < -18$ mag) SNe Ia from S-F and passive galaxies are distinct. In the V band, there is a difference of 0.4 ± 0.13 mag between the median (M_V) values of the 'normal' SN Ia population from passive and S-F galaxies. This is consistent with ($\sim 15 \pm 10$) per cent of 'normal' SNe Ia from S-F galaxies coming from an old stellar population.

Key words: supernovae: general.

1 INTRODUCTION

Type Ia supernovae (SNe Ia) are the best standardizable candles in the Universe. It is currently accepted that SNe Ia are produced from a carbon/oxygen white dwarf (WD) in a binary system. The three currently favoured progenitor scenarios are single degenerate (SD), double degenerate (DD) and collisions of C+O WDs in a triple system. In the SD scenario a C+O WD accretes material from a non-electron-degenerate companion star (Nomoto, Iwamoto & Kishimoto 1997). In the DD scenario two WDs merge after losing orbital angular momentum through the emission of gravitational waves (Iben & Tutukov 1984). Finally, the collision scenario is the head on collisions of two C+O WDs in a triple system (Rosswog et al. 2009; Katz & Dong 2012; Kushnir et al. 2013; Dong et al. 2015). For cosmological uses, SNe Ia can be put through intrinsic relations such as the width–luminosity relation (WLR) and the relation between SN Ia colour and luminosity (Phillips 1993; Riess, Press & Kirshner 1996; Riess et al. 1998). Applying these relations makes SNe Ia standardizable candles, reducing the scatter in their peak luminosity to ∼0.15 mag (e.g. Guy et al. 2007; Jha, Riess & Kirshner 2007; Conley et al. 2008).

To first order the luminosity of a SN Ia is driven by the amount of radioactive ^{56}Ni in the ejecta, and the relation between ^{56}Ni, luminosity and opacity determines the light-curve (LC) shape (Mazzali et al. 2007). However, spectroscopically no two SNe are exactly identical. They can have different spectral features, ionizations, velocities and ejecta abundances. There are currently at least six subclasses of SNe Ia: 'normal', 91T-like, 02cx-like, 91bg-like, 'super-Chandrasekhar' and SNe Ia-CSM.

SN 91T-like events, named after SN 1991T, are peculiar and overluminous. Spectroscopically they are characterized at early times by the weakness or absence of Ca II and Si II lines, and show very strong Si III lines. SN 1991T was ∼0.6 mag more luminous than normal SNe Ia (Sasdelli et al. 2014). It has been hypothesized that 91T-like events come from super-Chandrasekhar mass explosion mechanisms (Mazzali, Danziger & Turatto 1995; Fisher et al. 1999), but Sasdelli et al. (2014) find that a Chandrasekhar mass explosion is more suited to SN 1991T.

SN 1991bg and SN 91bg-like events have low luminosity, rapidly declining LCs, low ejecta velocities and a cool spectrum which is dominated by intermediate-mass elements (IME), as well as particularly strong O I and Ti II lines. They are also unusually red and are

★E-mail: c.ashall@2013.ljmu.ac.uk

underluminous by about ∼2 mag. The explosion mechanism of a 91bg-like SNe is a matter of debate, with options including DD explosions of WDs, sub-Chandrasekhar mass explosions triggered by detonation of the helium layer, or the collision of two WDs (Hillebrandt & Niemeyer 2000; Höflich et al. 2002; Mazzali & Hachinger 2012; Dong et al. 2015).

SN 2002cx-like events exhibit hot, SN 1991T-like pre-maximum spectra, a low, 91bg-like luminosity, a LC which is broad for the luminosity but dim for its shape, and low expansion velocities, roughly half of those of a normal SNe Ia (Li et al. 2003). These events are thought to come from the deflagration of a C+O WD, which only experiences partial burning that may (Sahu et al. 2008) or may not (Kromer et al. 2015) fully disrupt the WD.

Super-Chandrasekhar SNe Ia are very luminous, which suggests a large content and therefore a large ejected mass. They are thought to contain $>1.4\,M_{\odot}$ of ejecta, and probably come from a DD scenario (Howell et al. 2006; Yamanaka et al. 2009). However, they can also be explained by an 'interacting scenario', in which a SN Ia interacts with an H-/He-poor circumstellar medium (Hachinger et al. 2012).

Finally, SNe Ia-CSM show strong interaction with multiple thin H-rich CSM shells in the form of Hα emission and a blackbody-like continuum (Hamuy et al. 2003; Deng et al. 2004; Dilday et al. 2012; Silverman et al. 2013), and are probably SD SN Ia.

In modern times there has been a dramatic increase in SN data, which means that SNe Ia can be studied in more detail. One method to do this is by looking at individual objects, using a time series of spectra. By examining single objects one can look at the evolution of the abundances in the ejecta and their density profiles, therefore, placing constraints on their explosion properties. This approach can reveal intrinsic differences between two SNe which can appear to be photometrically similar, such as SNe 2011fe and 2014J (Ashall et al. 2014; Mazzali et al. 2014).

The increase in available data has also meant that large sample studies can now be performed, allowing one to gain more information about the variation in SN Ia properties. One way to separate SNe Ia is by host galaxy morphology. There have been many studies on SNe Ia differences depending on host galaxy type. It is known that faster declining and intrinsically dimmer SNe Ia are mostly found in passive galaxies (Hamuy et al. 1995, 1996). Peculiar subluminous 91bg-like SNe come from old stellar populations, at least 10 Gyr old (Howell 2001). Host stellar mass was also found to correlate with SN luminosities; more massive galaxies tend to host SNe Ia which have lower stretch (i.e. a larger rate of decline) than SNe in lower mass galaxies (Sullivan et al. 2010). The age or metallically of the progenitor may also contribute to SN Ia luminosities, but it is hard to observe these directly. Studying the early ultraviolet (UV) spectra of SNe Ia can let us infer information about the metallicity of the progenitor system (Lentz et al. 2000; Sauer et al. 2008; Mazzali et al. 2014). It is possible that SNe Ia that occur in galaxies with different star formation, age and dust properties may have intrinsically different luminosities (Childress et al. 2013; Rigault et al. 2013). It has also been shown that SNe Ia with a higher Si II 6355 line velocity tend to explode in more massive galaxies (Pan et al. 2015). This is not dissimilar from the result of Wang et al. (2013), who find that SNe Ia with high-velocity ejecta are more concentrated in inner, brighter regions of their host galaxy. Maguire et al. (2014) present a comparison of optical spectra with LC width information from Palomar Transient Factory (PTF), an untargeted transient survey. They find that on average SNe Ia with a broader LC shape have a larger contribution from the high-velocity component relative to the photospheric component in the Ca II near-infrared (NIR) feature.

A few studies have attempted to build the luminosity functions (LFs) of SNe Ia. Such information would be useful because it would make it possible to quantify the incidence of different subtypes of SNe Ia, and thus of their progenitor/explosion scenarios. Li et al. (2011) present a volume-limited LF from Lick Observatory Supernova. Search (LOSS), and find evidence for a difference in absolute magnitude between SNe Ia when these are separated into host galaxy bins of E-Sa and Sb-Irr. However, they do not correct for host galaxy extinction. Yasuda & Fukugita (2010) produce a LF of low-redshift SN discovered by Sloan Digital Sky Survey II (SDSS-II) supernova survey. They claim that the occurrence of SNe Ia does not favour a particular type of galaxy, but is predominantly dependent on the luminosity of the galaxy. They also claim that the rate of SNe Ia is higher by 31 ± 35 per cent in late-type than in early-type galaxies. Hicken et al. (2009) present a sample of 185 SNe Ia. They find that 91bg-like SNe Ia are distinct from other SNe Ia in their colour and LC shape–luminosity relation, and state that they should be treated separately in LC distance fitter training samples.

Although the use of SNe Ia as cosmological probes is well established, it is also known that a few events do not follow the normal 'rules' of SNe Ia. For example, PTF10ops (Maguire et al. 2011) was a subluminous SN Ia, but its LC had a normal width. 02cx-like events can also be broad in LC shape and intrinsically dim. Traditional LC fitting methods find it difficult to differentiate between colour and host galaxy extinction, so that, for example, a SN Ia which has a normal LC shape but is intrinsically red maybe mistaken for a SN which is normal but has more host galaxy extinction. Furthermore, for cosmological purposes, traditional methods exclude any intrinsically peculiar SNe Ia.

The objective of this paper is to include as many peculiar SNe Ia as possible, and hence examine their range and diversity. As there are many subclasses of SNe Ia, we take an approach different from LC template fitting analysis. Our analysis makes as few assumptions as possible so the intrinsic properties of these unusual SNe Ia can be examined. This allows for the possibility that SNe with the same LC shape can have intrinsically different properties. We achieve this by obtaining the distance to the SNe first, from data that do not use the SN as distance indicator, rather than obtaining the distance to the SNe from the LC shape and observed colour information. Although this method is possibly less accurate, it allows us to explore the full parameter space of SNe Ia, and is better at treating peculiar SNe Ia. Furthermore, our method is unique as we derive host galaxy extinction from the spectra rather than the photometry, which helps to break the colour-reddening degeneracy (Sasdelli et al. 2016), see Section 4. Because we cannot control the observed sample we cannot build a LF, but only a luminosity distribution (LD), which is however useful as all SNe used here are nearby, suggesting that the sample should be reasonably complete.

In this paper we carry out a large sample analysis, which primarily focuses on SN Ia LC properties, separated by host galaxy type. In Section 2 we discuss the data and methods used in this paper. Section 3 presents the observed SN Ia LDs and discusses the WLR. In Section 4 the data are corrected for host galaxy extinction, and separated by host galaxy type. In Section 5 we present the full LD. In Section 6 attempts to separate the distributions of SNe Ia from young and old stellar systems. The main discussion is provided in Section 7, and a short summary is presented in Section 8.

2 DATA AND METHOD

We have assembled a data set of 165 low-redshift, $z < 0.05$, SNe Ia with publicly available data. Their redshift distribution is shown in

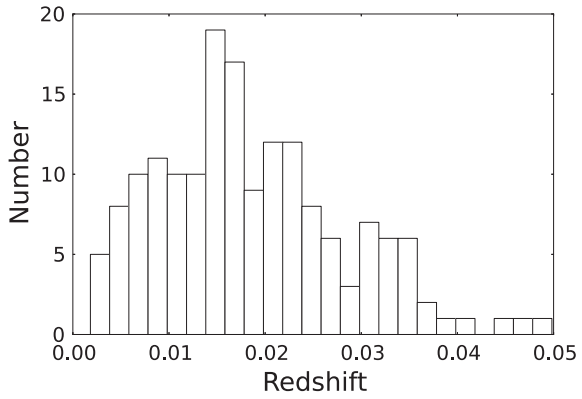

Figure 1. Redshift distribution of the SNe Ia used in this paper. The bin sizes are $z = 0.002$.

Table 1. Sources of the data.

Reference	Number of SNe Ia
Ganeshalingam, Li & Filippenko (2010)	102
Hicken et al. (2009)	24
Hicken et al. (2012)	18
Riess et al. (1999)	10
Individual papers[a]	11

Note. [a]See Appendix A.

Fig. 1. The photometric data in this paper come from a variety of public sources, see Table 1. The mean redshift of the sample is $z = 0.019$. When comparing SN Ia LCs and their derived parameters it is essential that they have sufficient temporal coverage, as overinterpolating or incorrectly extrapolating the data can cause incorrect results. All SNe in the data set used in this paper have good temporal coverage, at least six data points, from maximum to +15 d and at least one pre-maximum data point. The data used in this paper were published in the standard Johnson–Cousin filter system, and no filter conversions were carried out in this analysis. We use the *B*- and *V*-band filters for the analysis as this is where SNe Ia peak in flux; these bands are also historically the most often used, and therefore the best sampled. Most of the optical lines are within the *B* and *V* passbands, therefore, these bands are the best to study the diversity of SNe Ia. There is an obvious bias in our sample caused by the fact that most data were obtained by magnitude-limited surveys. However, we have used as many SNe Ia as possible to avoid small sample statistics. Because the data come from a range of sources it is not possible to carry out completeness corrections, therefore, in this work we produce LDs, which can show the diversity of SNe Ia, rather than LFs.

In order to avoid introducing any further biases, here we do not assume that two SNe Ia that have the same LC shape necessarily also have the same intrinsic luminosity and colours (unlike, e.g. Riess et al. 1996). This is done by first finding an independent distance to each SN and using that distance to determine the luminosity of the SN. The distances were derived using the local velocity field model of Mould et al. (2000), which takes into consideration the influence of the Virgo Cluster, the Great Attractor, the Shapley Supercluster and the cosmic microwave background (CMB). To verify the reliability of the distance measurements we checked against Cepheid distances for five SNe Ia which occurred in galaxies with Cepheid distance measurements. We found that the distances to the SNe Ia are consistent with the Cepheid distances (within 0.06 Mpc). The velocity field model requires a value of H_0. We use cosmological parameters which are consistent with Cepheid measurements, i.e. $H_0 = 73$ km s^{-1} Mpc^{-1}, $\Omega_m = 0.27$, $\Omega_\Lambda = 0.73$. It should be noted that a change in H_0 would cause a global shift in values, but it would not directly affect the results in this paper.

Before different SNe can be compared their photometry must be dereddened and converted to rest frame. All SNe were corrected for foreground Galactic extinction using the Schlafly & Finkbeiner (2011) map and assuming $R_v = 3.1$. The data were converted to the rest frame and *K*-corrections were applied. We used a time series of spectra of SN 2011fe (Mazzali et al. 2014) as a template to calculate the *K*-corrections, and carried out the corrections in accordance with Oke & Sandage (1968). Using SN 2011fe as a template is making an assumption about the spectral energy distribution (SED) of the SN, however, this affects the fluxes in our final results by less than 5 per cent in most cases. The *K*-corrections were applied to each SN at the corresponding redshift and epoch, using both the *B* and *V* bands.

Finding the host galaxy morphology of each SN in the data set is integral to our study. Host galaxy types were obtained from NED.[1] The data set was separated into two galaxy Hubble type bins, E-S0 (passive galaxies) and Sa-Irr [star-forming (S-F) galaxies]. We chose to separate our sample into these two bins only as the age of the stars is similar in the galaxies within each bin. Also, using more bins would significantly decrease the sample in each bin. E+S0 galaxies have an older stellar population with little or no star formation. Out of our sample of 165 SNe, 134 (82 per cent) SNe are from the Hubble Sa-Irr bin, 26 (13 per cent) are from the E+S0 bin, of which 17 (10 per cent) are from elliptical galaxies and nine (5 per cent) are from S0 galaxies. Finally, five SNe (3 per cent) are from galaxies whose host type could not be determined. Binning the SNe by host galaxy type does not decrease the sample as much as distinguishing by S-F rates or galaxy stellar mass.

We find that 133 (81 per cent) of the SNe were classified as spectroscopically 'normal', 14 (9 per cent) 91T or 99aa-like, 14 (8 per cent) at 91bg-like and four (2 per cent) as 02cx-like. Comparing this to the rates of SNe Ia from Li et al. (2011) (70 per cent normal, 15 per cent 91bg, 9 per cent 91T, 5 per cent 02cx) shows that the public data set has a bias of too many 'normal' SNe Ia and fewer dimmer SNe. The lack of 91bg-like events in our sample could be due to their short rise time, which makes them harder to detected before maximum light. SNe without maximum light information would be excluded from the sample in this paper. Additionally, 91bg-like SNe are dimmer events and are therefore affected by Malmquist bias. This does raise the issue that if one wants a true representation of the intrinsic properties of SNe Ia, a very high cadence, deep and volume-limited survey is required, as well as a lot of ground-based spectroscopic follow up, however, this is not available. It should be noted that the host galaxy subtraction from Li et al. (2011) excludes the central 2.4–3.2 arcsec region of the host galaxies, so the true rate may differ from theirs since they exclude SNe Ia from the centre of galaxies.

SNe Ia photometry, to first order, can be analysed using two parameters, the decline rate or stretch of the LC and the colour correction of the SNe. This is traditionally done using LC template fitters, and is therefore based on existing assumptions, data and

[1] NASA/IPAC Extragalactic Database (NED).

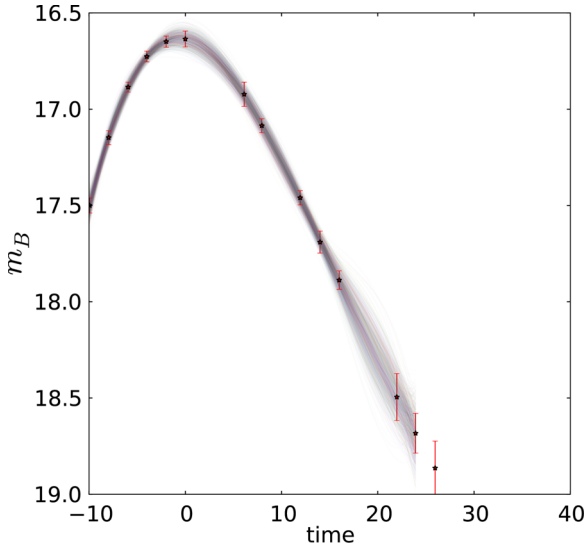

Figure 2. An example of the fitting procedure, the *B*-band LC of SN 2000dn. The red points are the photometry and the shaded area is the 1000 LCs derived from these photometry points, as explained in Section 2.1.

templates. In reality SNe Ia are a far more diverse group than these LC fitters can assume, as their spectra show. Therefore, we chose to make no prior assumptions in our LC fitting process, but rather to produce our own method of fitting the data. In this section we explain how the photometry is fitted and how we calculate the errors. The LCs are produced by using a smoothed cubic spline, implementing the PYTHON module UNIVARIANT SPLINE, on the photometry which has been *K*-corrected and dereddened for foreground Galactic extinction. We use these values as the final values of the apparent magnitude and LC shape, as measured by the parameter $\Delta m_{15}(B)$, the difference in magnitude between maximum and +15 d (Phillips 1993). This process was carried out for both the *B* and *V* bands. The two spline fits were subtracted to obtain the $B - V$ curve, and from this the colour at *B* maximum, $(B - V)_{B_{\max}}$, was obtained. The distance modulus was used to obtain the absolute magnitudes M_B and M_V of all SNe in the sample.

To compute the errors on the apparent magnitude and Δm_{15} we treat all of the photometric errors as Gaussians. We randomly vary each photometric point, in accordance to the weighting of a Gaussian. From this new LCs are produced, using the method discussed above. This was done 1000 times per SN, and the standard deviation in the spread of values is taken as the errors on apparent magnitude and $\Delta m_{15}(B)$. As an example of this process, Fig. 2 shows the photometry and fitted LCs for SN 2000dn. The peak apparent magnitude for SN 2000dn is 16.63 ± 0.03 mag and the decline rate $\Delta m_{15}(B) = 1.11 \pm 0.07$ mag. We only fitted the LC up to 30 d past *B*-band maximum, as we are not analysing late time photometry in this paper. The plot demonstrates that there is a larger spread in values when the errors on the photometry are larger. On the other hand, high cadence photometry reduces the errors. As we obtained SNe from multiple sources we cannot distinguish between systematic errors which could cause a global shift in the LC, and errors such as poor host galaxy subtraction, which would affect the shape of the LC. Therefore the errors of our fits could be overestimated if the errors on the photometry include systematics. For more information on the quality of the LC fit the reader is referred to Appendix B.

3 LUMINOSITY DISTRIBUTION

3.1 *B* and *V* luminosity distributions

The *B*-band absolute magnitude and decline rate distributions of the SNe in our sample before correction for reddening are shown in the top panels of Fig. 3. The bin sizes are 0.2 for M_B and 0.1 mag for $\Delta m_{15}(B)$. The mean *B*-band absolute magnitude of the sample is $\bar{M}_B = -18.58 \pm 0.07$ mag, see Table 2, and the sample ranges from −19.8 to −15.6 mag. There is no definitive peak in absolute magnitude in this distribution, which is due to the missing correction for host galaxy extinction and to the 'tail' of subluminous SNe. The distribution in $\Delta m_{15}(B)$ is bimodal, with two peaks at 0.9–1.0 and 1.7–1.8 mag. A Gaussian-mixture modelling test (GMM; Muratov & Gnedin 2010) was run to evaluate the likelihood that a bimodal distribution is preferred over a unimodal one. It is found that for $\Delta m_{15}(B)$ a bimodal distribution is preferred: the probability that the $\Delta m_{15}(B)$ distribution is unimodal is less than 0.1 per cent. The bimodal distributions are assumed to be Gaussians. Out of the 165 SNe Ia in the sample, the test places 135.3 ± 20.8 SNe (82 per cent) in a Gaussian with mean decline rate $\Delta m_{15}(B) = 1.034 \pm 0.035$ mag and standard deviation 0.207 ± 0.032 mag, and 29.7 ± 20.8 SNe (18 per cent) in a Gaussian with mean decline rate 1.713 ± 0.131 mag and standard deviation 0.164 ± 0.080 mag. This is more than the fraction of 91bg-like SNe. The bimodal distribution could be due to the presence of sub-Chandrasekhar-mass events with large $\Delta m_{15}(B)$ (e.g. Mazzali et al. 2011; Mazzali & Hachinger 2012), or to delayed-detonation explosions with a range of transition densities from deflagration to detonation: Höflich et al. (2002) find that for a range of smoothly distributed transition densities there is a lack of SNe Ia with ^{56}Ni mass between 0.15 and 0.25 $M_\odot$. This gap corresponds to the lack of SNe Ia at $\Delta m_{15}(B) = 1.6$ mag seen in Fig. 3.

SNe in the trough between the two peaks are typically classified as 'transitional', with examples being SNe 2004eo (Pastorello et al. 2007) and 2012ht (Yamanaka et al. 2014). Transitional SNe bridge the gap between 'normal' and 91bg-like SNe Ia. The ejected ^{56}Ni mass ($M_{\rm Ni}$) of transitional SNe Ia lie near the lower limit of the $M_{\rm Ni}$ distribution of normal SNe Ia. There is still a lack of published literature on transitional SNe Ia. It is these objects which could help define whether 91bg-like SNe Ia arise from a separate population or there is a smooth distribution of properties SNe Ia. iPTF13ebh, SN 1986G and SN 2003hv are all classified as transitional SNe Ia. None of these events follows the normal paradigm of SNe Ia. SN 2003hv may have less mass in the inner layers of the ejecta than Chandrasekhar-mass density profiles predict: synthetic nebular models were unable to produce the high Fe III/Fe II ratio in the optical spectrum along with the low infrared flux using a W7 density profile (Leloudas, Stritzinger & Sollerman 2009), but a lower mass yielded good results (Mazzali et al. 2011). SN 1986G was the first reported SN of this type. It was spectroscopically similar to subluminous SNe, showing a (weaker) Ti II feature, a large ratio of the Si II lines (Nugent et al. 1995; Hachinger, Mazzali & Benetti 2006) and narrow unblended lines in the Fe ∼ 4800 Å feature (Phillips et al. 1987). iPTF13ebh showed several strong NIR C I lines in the early time spectra, but no strong C I lines in the optical (Hsiao, Burns & Contreras 2015).

It should be noted that Maguire et al. (2014) do not find a bimodal distribution in Δm_{15} when they convert their values of stretch to Δm_{15}. This may indicate that the double-peak distribution in Δm_{15} could be a selection effect. However, it is unclear how reliable the conversion from stretch to $\Delta m_{15}(B)$ is. Furthermore, Maguire et al.

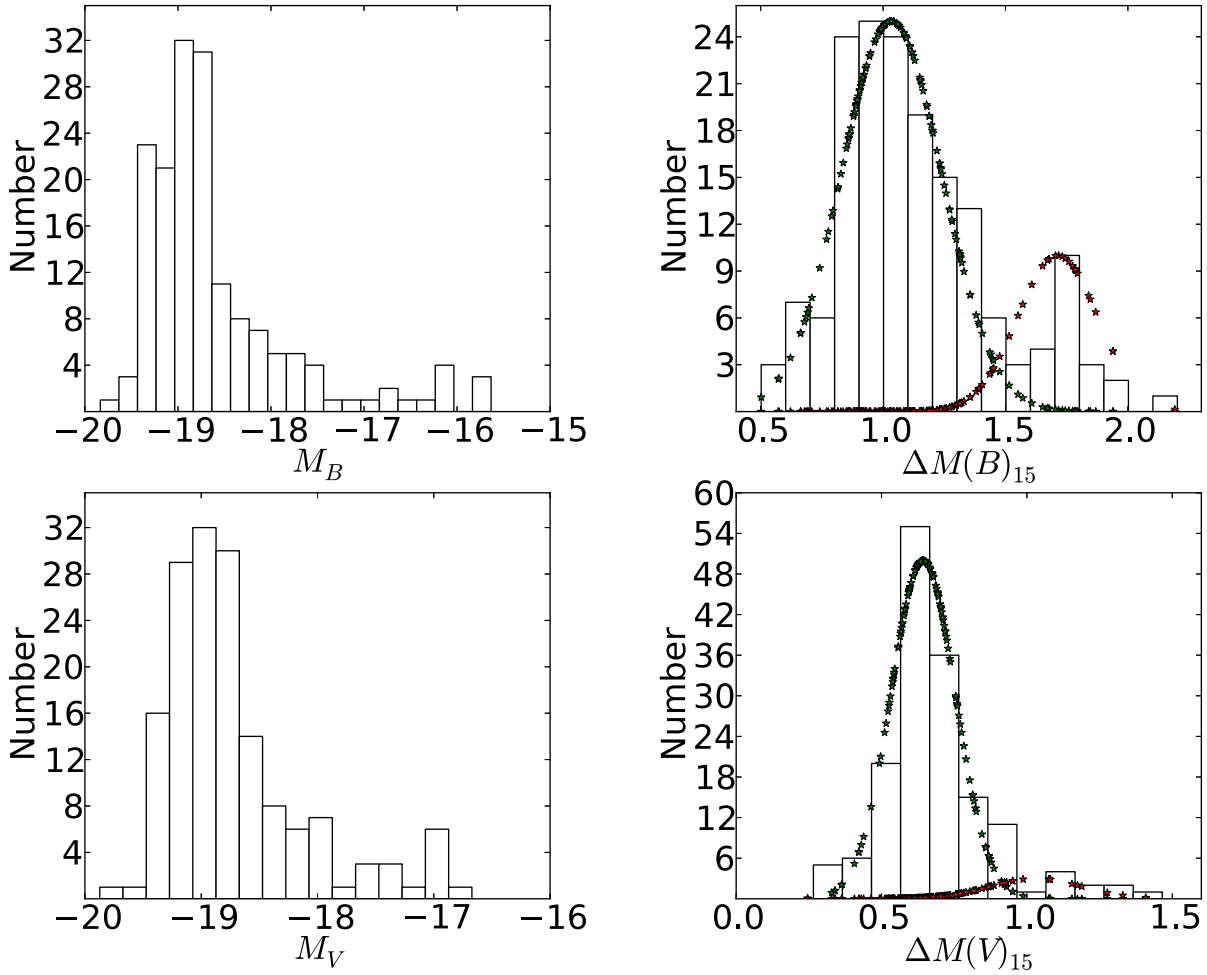

Figure 3. The LDs and Δm_{15} distributions of the SNe sample before correction for reddening. Top: the left-hand plot is a distribution of *B*-band absolute magnitude, and the right-hand plot is the distribution of $\Delta m_{15}(B)$. Bottom: the left-hand plot is a distribution of *V*-band absolute magnitude, and the right-hand plot is the distribution of $\Delta m_{15}(V)$. In these plots the SNe have not been corrected for host galaxy extinction. The stars in two right-hand panels are the Gaussians calculated from the GMM tests.

Table 2. Statistics of the data, not corrected for host galaxy extinction has been applied.

	All	Active	Passive	E	S0
Amount of SNe	165	134	26	17	9
$\overline{M_B}$	-18.58 ± 0.07	-18.63 ± 0.07	-18.29 ± 0.21	-18.29 ± 0.24	-18.30 ± 0.39
σM_B	0.82	0.77	1.06	0.99	1.17
$\overline{\Delta M_{15} B}$	1.14 ± 0.03	1.11 ± 0.03	1.29 ± 0.08	1.30 ± 0.10	1.28 ± 0.12
$\sigma \Delta M_{15} B$	0.32	0.30	0.39	0.40	0.35
$\overline{M_V}$	-18.72 ± 0.05	-18.75 ± 0.05	-18.52 ± 0.15	-18.50 ± 0.17	-18.56 ± 0.29
σM_V	0.61	0.58	0.76	0.71	0.86
$\overline{\Delta m_{15} V}$	0.68 ± 0.01	0.67 ± 0.01	0.77 ± 0.05	0.79 ± 0.06	0.74 ± 0.07
$\sigma \Delta m_{15} V$	0.18	0.16	0.25	0.25	0.22
$\overline{(B-V)}^a$	0.11 ± 0.02	0.11 ± 0.02	0.17 ± 0.06	0.16 ± 0.07	0.20 ± 0.10
$\sigma (B-V)^a$	0.25	0.24	0.29	0.29	0.29

Note. [a]At *B* max.

(2014) use data from a flux limited survey, and therefore the difference between their distribution and ours could stem from the lack of observed SN 91bg-like events in their sample. Burns et al. (2014) state that $\Delta m_{15}(B)$ is an unreliable parameter for fast declining SNe Ia with $\Delta m_{15}(B) > 1.7$ mag, because for these SNe there is a degeneracy between LC shape and $\Delta m_{15}(B)$. Here, however, $\Delta m_{15}(B)$ is used only to discriminate between normal and subluminous SNe Ia, which is sufficient for our analysis.

The lower part of Fig. 3 presents the *V*-band absolute magnitude and $\Delta m_{15}(V)$ distributions. Bin sizes are again 0.2 and 0.1 mag, respectively. The mean M_V value is $\bar{M}_V - 18.72 \pm 0.05$ mag, while $\bar{\Delta m_{15}}(V) = 0.68 \pm 0.01$ mag. We find no statistical evidence that

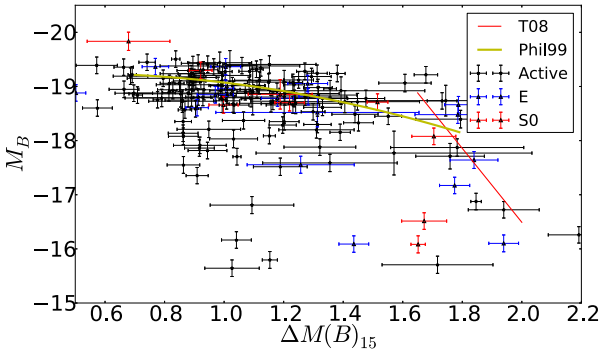

Figure 4. The *B*-band WLR before reddening correction. The black points are SNe from S-F galaxies, the blue points are SNe from E galaxies and the red points are SNe Ia from S0 galaxies. The yellow line is the WLR given in Phillips et al. (1999), and the red line is the relation given for the subluminous tail from Taubenberger et al. (2008).

the distribution in $\Delta m_{15}(V)$ is bimodal. Although not statistically significant, a bimodal $\Delta m_{15}(V)$ distribution has been plotted in Fig. 3 (bottom left-hand panel). The two Gaussians have mean $\Delta m_{15}(V)$ of 0.642 ± 0.015 and 0.999 ± 0.201 mag and standard deviations of 0.106 ± 0.031 and 0.166 ± 0.067 mag, respectively.

The standard deviation in absolute magnitude, see Fig. 3, is less in the *V* band (0.61 mag), than in the *B* band (0.82 mag). This is partly caused by the fact that the *B* band is more affected by extinction. It could also be caused by some SNe Ia having broad, a high velocity Ca II feature at ∼3800 Å or different amount of line blanketing in the UV, although the latter will not be the largest contributor to the difference.

3.2 Width–luminosity relation

Type Ia SNe are known to show an inverse correlation between their absolute magnitude and the rate at which they decline, Δm_{15}. This is as the widths of the LCs are a function of ejecta mass, ^{56}Ni mass, kinetic energy and opacity (Mazzali et al. 2007). The WLR relationship was first published by Phillips (1993), and extended by Phillips et al. (1999) and then Taubenberger et al. (2008). Fig. 4 shows this relation within the context of our work. It is clear that there is an underlying correlation ('the Phillips Relation') with some scatter. The relation from Phillips et al. (1999) is plotted in Fig. 4 to show this. SNe Ia with low luminosity but $\Delta m_{15}(B) < 1.6$ are likely to be affected by host galaxy extinction, but we cannot determine this using only this plot. Faster declining SNe tend to come from passive galaxies and are less affected by extinction. Therefore, the 'tail' in the WLR, which was first pointed out by Taubenberger et al. (2008), is likely to be intrinsic, and not the effect of extinction. Their relation for the subluminous tail is also plotted in Fig. 4. Furthermore, there is a dearth of SNe at $\Delta m_{15}(B) \sim 1.6$ mag, where the SNe transition from 'normal' to subluminous. Interestingly this gap is where the two relations from Phillips et al. (1999) and Taubenberger et al. (2008) meet.

To overcome the effect of extinction, one could select only SNe with a very small colour term, $(B - V)_{\rm Bmax} < 0.01$, as they are thought to be less affected by host galaxy extinction. The top panel in Fig. 5 shows that the scatter in the WLR plot is indeed reduced when only these SNe are selected. We obtain a second-order polynomial line of best fit, shown as the blue line in Fig. 5, given by

$$M_B = 0.252\Delta m_{15}(B)^2 - 0.015\Delta m_{15}(B) - 19.31. \quad (1)$$

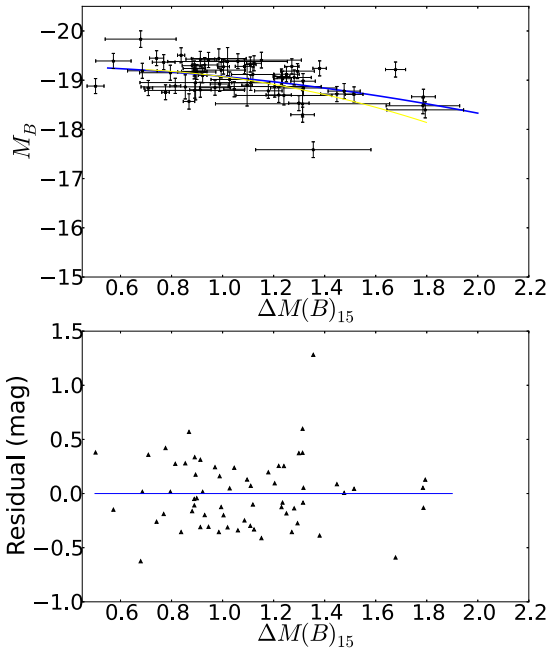

Figure 5. Top: the WLR before reddening correction including only SNe with $(B - V)_{B_{\rm max}} < 0.01$. The blue line of best fit is a second-order polynomial. The yellow model is the line of best fit from Phillips et al. (1999). Bottom: the residuals of the WLR above as a function of $\Delta m_{15}(B)$.

However, this approach eliminates any intrinsically red or unusual SNe Ia. The bottom plot in Fig. 5 shows the residuals from this fit; the mean residual is 0.22 mag. The reduced χ^2 of the fit is 3.3. When compared to the fit from Phillips et al. (1999) (red model in the top panel of Fig. 5), we find a similar result, although our fit is not as tight. The SN which sits clearly off the Phillips relation, with a value of $M_B > -18$ mag is SN 2008cm. SN 2008cm has been rejected in cosmological studies for being an outlier (Rest, Scolnic & Foley 2014). This demonstrates that LCs alone do not contain enough information to differentiate between types of SNe Ia.

4 CORRECTION FOR HOST GALAXY EXTINCTION

The intrinsic colours of SNe Ia change over time because of the changing properties of the ejecta. For less luminous SNe this change is over a shorter time-scale than for more slowly declining SNe. It is observationally difficult to distinguish between intrinsic colour changes and reddening due to dust between the SNe and the observer. Determining this is central to the full understanding of the nature of SNe Ia, but it is not trivial. Several studies tried to estimate SN Ia colour. The Lira law (Phillips et al. 1999) found that the $B - V$ colours of SNe Ia, at all decline rates, evolve in a nearly identical way, from +30 to +90 d past *V* maximum. It has also been shown that high- and normal-velocity (NV) SNe exhibit significant discrepancies in $B - V$ and $B - R$, but not in other colours (Mandel, Foley & Kirshner 2014).

Spectral properties such as equivalent widths (EW) can be used as indicators to attempt to distinguish between colour and host galaxy extinction. EWs are not affected by extinction, and there are intrinsic relationships between the EW of certain lines and the SN LC parameters, such as between EW(Si II 5972) and $\Delta m_{15}(B)$ (Nugent et al. 1995; Hachinger et al. 2006). When trying to obtain extinction from estimates of reddening, it is important that the correct

value of R_v (the total to selective extinction) is used. In the Milky Way the average value of R_v is 3.1, but it varies depending on the region observed. For SNe Ia very low values of R_v have sometimes been reported, ranging from 1.1 to 2.2 (Tripp 1998; Kessler, Becker & Cinabro 2009; Folatelli, Phillips & Burns 2010; Guy et al. 2010). Chotard, Gangler & Aldering (2011) derived a larger value of $R_v = 3.1$, which is consistent with the Milky Way value (Cardelli, Clayton & Mathis 1989). Sasdelli et al. (2016) used time series of SNe Ia spectra in derivative space, which is not affected by poor calibration, to explore host galaxy extinction, and found that $R_v = 2.9 \pm 0.3$ fits the data the best, and is also consistent with the MW value.

From the WLR in Fig. 4, it is not possible to tell how much of the scatter is intrinsic and how much is due to extinction, since SNe Ia are not perfectly homogeneous. For almost all astronomical data, correction for both Galactic and host extinction is important, especially when comparing objects. Sasdelli et al. (2014) attempted to break the colour-reddening degeneracy using spectroscopic time series as predictor variables of the intrinsic colour. They built a metric space for SNe Ia independent of extinction using principal component analysis (PCA). The intrinsic spectral evolution of the SNe Ia is represented by a five-dimensional feature space. This space does not include dust extinction. Two intrinsically similar SNe with different extinction have similar projections in this feature space. Sasdelli et al. (2014) use this feature space to predict the $B - V$ colour of SNe using a partial least square (PLS) regression. Only the intrinsic part of the $B - V$ colour can be predicted by PLS. The difference between the predicted intrinsic colour and the observed $B - V$ colour can then be interpreted as due to dust extinction. This yields estimates of $E(B - V)$ for the individual SNe. With this host galaxy extinction information we can examine the intrinsic properties of SNe Ia.

In this section we apply a correction for host galaxy extinction based on the method of Sasdelli et al. (2016) and use the values of $E(B - V)$ thus derived. This method removes spectroscopically peculiar SNe Ia that are underrepresented in the data, and therefore can bias our sample towards normal and luminous SNe Ia. We correct the extinction using the Cardelli–Clayton–Mathis (CCM) law (Cardelli et al. 1989) with $R_v = 2.9$, and use the approximation

$$\Delta m_{15}(B)_{\rm true} = \Delta m_{15}(B)_{\rm obs} + 0.1 \times E(B - V) \quad (2)$$

to correct $\Delta m_{15}(B)$ for extinction. $\Delta m_{15}(V)$ has not been corrected for extinction as the effect is negligible in the V band (Phillips et al. 1999).

As the sample size is reduced in this section of the analysis, we first verify the main properties of the SN sample before and after host galaxy extinction correction is applied, in order to determine whether the reduced sample is selected randomly from the larger one or it is biased towards normal SNe Ia by the selection process. For the sample before correction, $\bar{M}_B = -18.66 \pm 0.07$ mag, which is comparable to -18.58 ± 0.07 mag from the larger uncorrected sample, see Tables 3 and 2 respectively. The mean $\Delta m_{15}(B)$ values from the two samples are also similar, 1.14 ± 0.03 and 1.11 ± 0.03 mag for the larger and smaller samples, respectively. The mean M_V values were also found to be similar, -18.72 ± 0.05 and -18.77 ± 0.05 mag for the larger and smaller samples, respectively. Out of the 56 SNe Ia which were removed from the sample two were 91bg-like, four were 91T-like, 47 were normal SNe Ia. These SNe were rejected as they had insufficient spectral coverage, so it is not possible to tell if they have a peculiar spectral evolution. The other three of the 56 had to be removed from the sample for being spectroscopically peculiar. These were 2005hk (a 2002cx-like SN), 2004dt (a highly polarized SN; Altavilla et al. 2007) and 1999cl (a highly extinguished SN).

4.1 Host galaxy extinction

Fig. 6 shows the amount of host extinction for each galaxy type derived with the method of Sasdelli et al. (2016). The top left-hand plot shows how the LD of SNe Ia from S-F galaxies changes when host galaxy extinction is corrected for. The top right-hand plot shows that there is a large difference between the values of M_B before and after extinction correction. If there was no correction for extinction all data points would fall on a linear relation. This is however not the case: 67 per cent of SNe Ia from S-F galaxies are affected by detectable amounts of host galaxy extinction. The average $E(B - V)$ of all SNe Ia from S-F host galaxies is 0.130 ± 0.023 mag. In contrast, only 43 per cent of the SNe Ia from passive galaxies are affected by detectable amounts of host galaxy extinction, as would be expected due to the lack of dust in early-type galaxies. Their mean $E(B - V) = 0.040 \pm 0.013$ mag. Therefore on average SNe from passive galaxies have almost negligible host galaxy extinction. The average change in absolute B magnitude for SNe Ia from S-F

Table 3. Statistics of data before correction for host galaxy extinction. The data used in this table are a subset of the full sample.

	All	S-F	Passive	E	S0
Amount of SNe	109	89	16	11	5
$\overline{M_B}$	-18.66 ± 0.07	-18.70 ± 0.08	-18.42 ± 0.23	-18.48 ± 0.28	-18.29 ± 0.43
σM_B	0.74	0.71	0.94	0.92	0.97
MedianM_B	-18.85 ± 0.09	-18.88 ± 0.09	-18.80 ± 0.29	-18.81 ± 0.35	-18.71 ± 0.54
$\overline{\Delta m_{15} B}$	1.11 ± 0.03	1.08 ± 0.03	1.29 ± 0.10	1.24 ± 0.13	1.40 ± 0.13
$\sigma \Delta m_{15} B$	0.32	0.29	0.39	0.42	0.30
$\overline{(B - V)}$	0.097 ± 0.022	0.095 ± 0.025	0.132 ± 0.062	0.104 ± 0.070	0.193 ± 0.118
$\sigma(B - V)$	0.233	0.233	0.247	0.234	0.263
Median$(B - V)$	0.040 ± 0.03	0.040 ± 0.03	0.039 ± 0.08	0.030 ± 0.09	0.077 ± 0.15
$\overline{M_V}$	-18.77 ± 0.05	-18.81 ± 0.06	-18.60 ± 0.17	-18.63 ± 0.20	-18.53 ± 0.31
σM_V	0.55	0.52	0.68	0.68	0.68
Median M_V	-18.88 ± 0.07	-18.90 ± 0.07	-18.83 ± 0.21	-18.86 ± 0.26	-18.74 ± 0.38
$\overline{\Delta m_{15} V}$	0.67 ± 0.02	0.65 ± 0.02	0.80 ± 0.06	0.79 ± 0.09	0.82 ± 0.08
$\sigma \Delta m_{15} V$	0.19	0.16	0.26	0.29	0.17

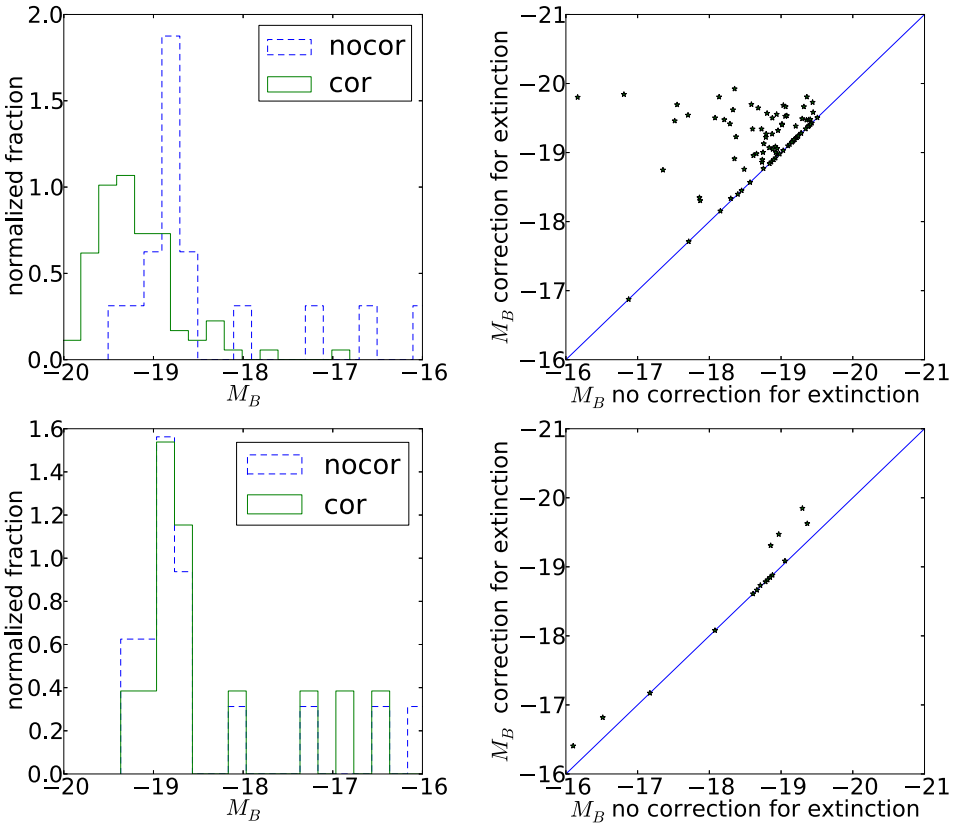

Figure 6. Top: left: the M_B LD of the SN Ia from S-F galaxies, before and after correction for extinction. Right: compares the values of M_B, again before and after correction for extinction, for SNe from S-F galaxies. Bottom: left: the M_B LD of the SNe Ia from passive galaxies, before and after correction for extinction. Right: M_B, before and after correction for extinction, for SNe from passive galaxies.

galaxies is 0.50 mag, compared to 0.15 mag for SNe from passive galaxies.

4.2 Luminosity distribution

The top left-hand panel of Fig. 7 shows the M_B distribution of the SNe after correction for host galaxy extinction. The distribution has mean $\bar{M}_B = -19.09 \pm 0.06$ mag and a standard deviation $\sigma(M_B) = 0.62$ mag. The LD consists of a 'normal' distribution of SNe Ia and of a subluminous 'tail' comprising faster declining SNe Ia. A similar result is found in the V band (Fig. 7, lower left), where the distribution has mean $\bar{M}_V = -19.10 \pm 0.05$ mag and $\sigma(M_V) = 0.52$ mag. From Fig. 7 it is apparent that when corrected for extinction 'normal' SNe Ia lie within the range $-20 > M_B > -18$, and similarly for M_V.

The right-hand side of Fig. 7 shows the distribution of decline rates. In the B band, the distribution has a mean $\Delta m_{15}(B) = 1.12 \pm 0.03$ mag and a standard deviation of 0.32. A bimodal distribution is still visible in $\Delta m_{15}(B)$ showing a lack of 'transitional' objects. Table 4 contains the statistics of the SNe Ia sample when corrected for extinction.

4.3 LD by host galaxy type

We separated the SNe by host galaxy type, as discussed in Section 2. Fig. 8 shows the LDs of SNe Ia separated by host galaxy type, after correction for extinction. In the B-band, SNe from S-F galaxies have $\bar{M}_B = -19.20 \pm 0.05$ mag, while SNe from passive galaxies have $\bar{M}_B = -18.57 \pm 0.24$ mag, which is 0.63 ± 0.24 mag dimmer. In the V band, SNe Ia from S-F galaxies have $\bar{M}_V = -19.19 \pm 0.05$ mag, while SNe from passive galaxies have $\bar{M}_V = -18.71 \pm 0.18$ mag. The difference in V-band average absolute magnitude is 0.48 ± 0.24 mag. Faster declining SNe tend to favour passive galaxies, which is expected as subluminous SNe tend to favour old stellar populations (Howell 2001). The mean $\Delta m_{15}(B)$ for SNe from passive galaxies is 1.29 ± 0.10 mag, compared to 1.10 ± 0.03 mag for SNe Ia from S-F galaxies.

We ran K–S tests on the distributions from each host galaxy, see Table 5. The probability that the M_B samples come from the same parent distribution is less than 0.1 per cent. There is marginal evidence for a difference between the $\Delta m_{15}(B)$ distributions, with a 12 per cent probability that they came from the same parent sample. When we ran these tests on the V band, we found that the M_V distributions had less than a 0.4 per cent probability of coming from the same parent distribution.

The mean colour term for SNe Ia after correction for host galaxy extinction is -0.008 ± 0.013 mag. SNe Ia from S-F galaxies have an average $(B-V)_{B_{\max}} = -0.025 \pm 0.010$ mag. This is 0.12 ± 0.06 mag bluer than for SNe Ia from passive galaxies, which have an average colour term of 0.095 ± 0.060 mag. This demonstrates that SNe Ia from S-F galaxies are intrinsically bluer than those from passive galaxies.

4.4 WLR after extinction correction

Fig. 9 shows the WLR of the SNe Ia in our sample after correction for host galaxy extinction. There is a larger intrinsic scatter in this WLR compared to when only SNe with $(B-V)_{B_{\max}} < 0.01$ mag

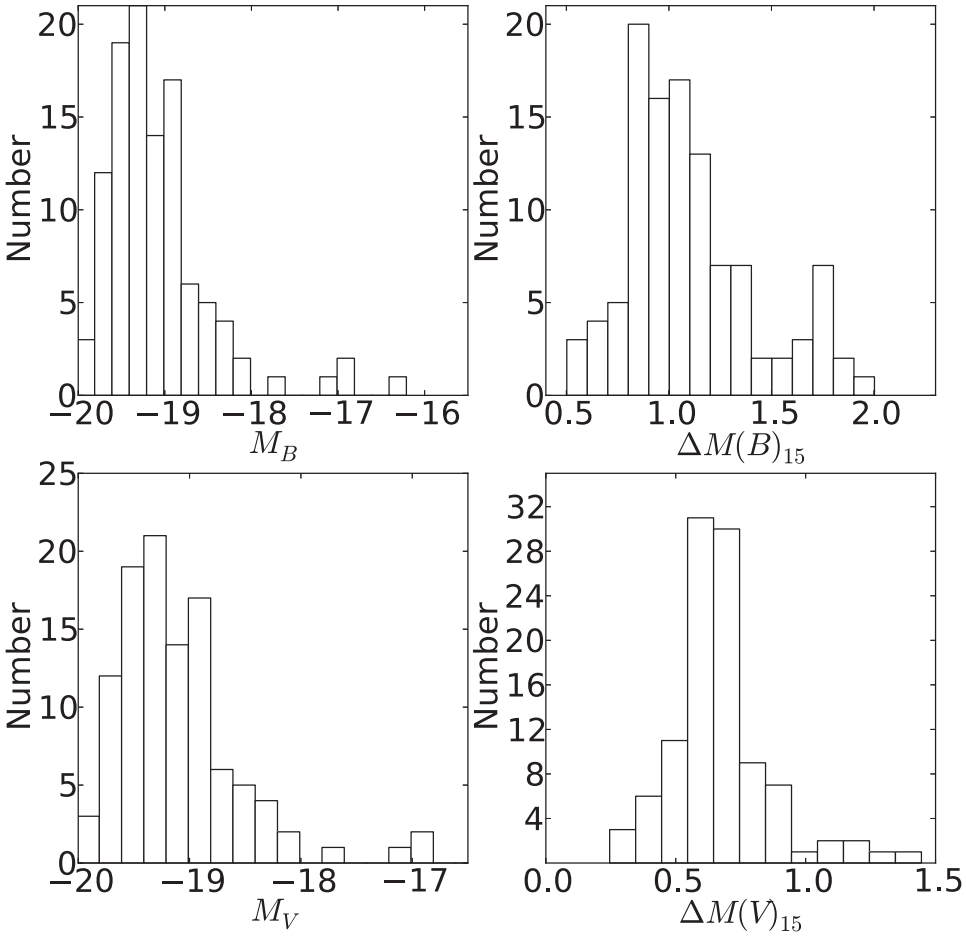

Figure 7. Top: B-band LD, corrected for host galaxy extinction. The bin sizes are 0.15 and 0.1 mag for the M_B and $\Delta m_{15}(B)$ plots, respectively. Bottom: V-band LD, corrected for host galaxy extinction. The bin sizes are 0.15 and 0.1 mag for the M_V and $\Delta m_{15}(V)$ plots, respectively.

Table 4. Statistics of the data after correction for host galaxy extinction.

	All	S-F	Passive	E	S0
Amount of SNe	109	89	16	11	5
$\overline{M_B}$	-19.09 ± 0.06	-19.20 ± 0.05	-18.57 ± 0.24	-18.58 ± 0.27	-18.56 ± 0.47
σM_B	0.62	0.49	0.96	0.91	1.05
MedianM_B	-19.22 ± 0.07	-19.27 ± 0.07	-18.80 ± 0.30	-18.81 ± 0.34	-18.73 ± 0.59
$\overline{\Delta m_{15} B}$	1.12 ± 0.03	1.10 ± 0.03	1.29 ± 0.10	1.24 ± 0.13	1.41 ± 0.13
$\sigma \Delta m_{15} B$	0.32	0.29	0.39	0.42	0.30
$\overline{(B-V)}$	-0.008 ± 0.013	-0.025 ± 0.010	0.095 ± 0.060	0.079 ± 0.067	0.129 ± 0.119
$\overline{(B-V)}$	0.135	0.097	0.239	0.223	0.266
Median$(B-V)$	-0.029 ± 0.02	-0.034 ± 0.01	-0.007 ± 0.07	-0.019 ± 0.08	0.004 ± 0.15
$\overline{M_V}$	-19.10 ± 0.05	-19.19 ± 0.05	-18.71 ± 0.18	-18.71 ± 0.20	-18.73 ± 0.34
σM_V	0.52	0.45	0.70	0.68	0.76
Median M_V	-19.17 ± 0.06	-19.23 ± 0.06	-18.83 ± 0.22	-18.86 ± 0.26	-18.75 ± 0.43
$\overline{\Delta m_{15} V}$	0.67 ± 0.02	0.65 ± 0.02	0.80 ± 0.07	0.79 ± 0.087	0.82 ± 0.08
$\sigma \Delta m_{15} V$	0.19	0.16	0.26	0.29	0.17
$\overline{E(B-V)}$	0.114 ± 0.019	0.130 ± 0.023	0.040 ± 0.013	0.026 ± 0.013	0.070 ± 0.026
$\sigma E(B-V)$	0.20	0.21	0.05	0.04	0.06

are used. This indicates that the parameter space that SNe Ia can fill is much larger than originally thought. This is the result of the breaking of the colour/extinction degeneracy by the method of Sasdelli et al. (2016). The bulk of 'normal' SNe Ia lie in a range of ∼1.5 mag, rather than showing a tight correlation between LC shape and absolute magnitude. Among SNe with $\Delta m_{15}(B) > 1.6$ mag, the subluminous tail dominates. This is where transitional SNe, with $1.6 < \Delta m_{15}(B) < 1.8$ mag, and subluminous SNe Ia, with $\Delta m_{15}(B) > 1.8$ mag, are. These SNe Ia are far more diverse in properties than 'normal' ones. In Fig. 9 the highlighted green mark located

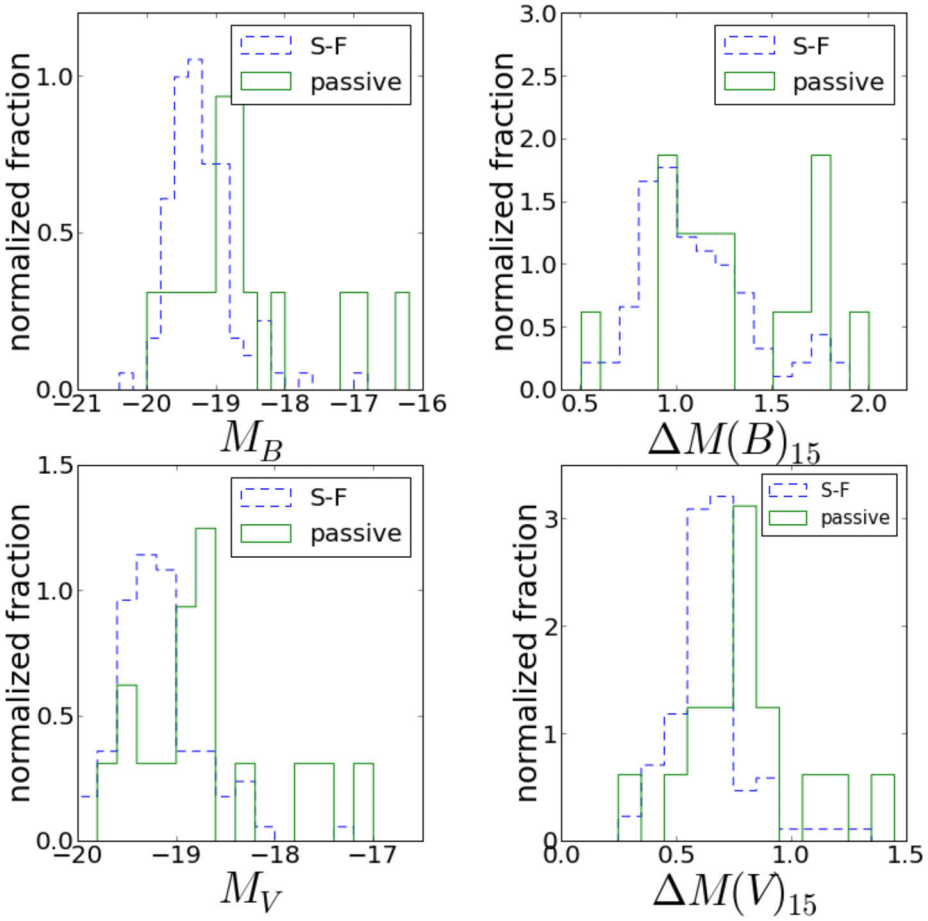

Figure 8. SNe Ia separated by host galaxy type, after correction for host galaxy extinction. Blue shows SNe Ia from S-F galaxies and green is SNe Ia from passive galaxies.

Table 5. K–S tests for SNe with different types of host galaxies, after correction for host galaxy extinction.

Compared distributions	Value used	*P* value
SNe active versus SNe passive	$M(B)_{15}$	0.001
SNe active versus SNe passive	$\Delta M(B)_{15}$	0.118
SNe active versus SNe passive	M_V	0.004

well above the WLR is SN 2003cg. This is the SN with the largest extinction, $E(B-V) = 1.026$ mag. Elias-Rosa et al. (2006) find that SN 2003cg has an anomalous extinction with $R_v = 1.80 \pm 0.19$ mag. SNe with very high extinction may require a different reddening law, but this is the only case in our sample for which this occurs. For more information on highly extinguished objects see Sasdelli et al. (2016).

5 FULL LUMINOSITY DISTRIBUTION

It is apparent that SNe Ia from passive galaxies suffer only from negligibly from host galaxy extinction, with 57 per cent of SNe Ia from passive galaxies having no detectable host galaxy extinction. The mean $E(B-V)$ for SNe Ia from passive galaxies is 0.04 ± 0.013 mag. In this section we use the sample of 105 SNe Ia which could be corrected for host galaxy extinction, and add back in the 10 SNe Ia from passive galaxies for which host galaxy extinction could not be derived. We do this to avoid small sample statistics.

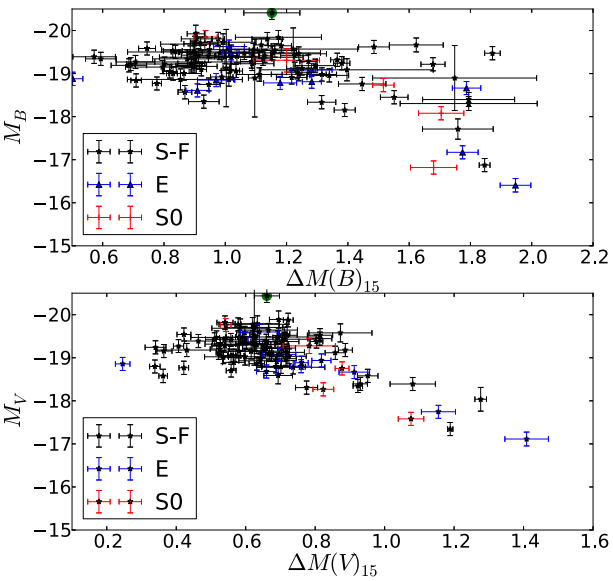

Figure 9. The WLR corrected for host galaxy extinction. The black points are SNe from S-F galaxies, the blue are points are SNe from elliptical galaxies and the red points are SNe Ia from S0 galaxies. The green point is SN2003cg. Top: *B* band. Bottom: *V* band.

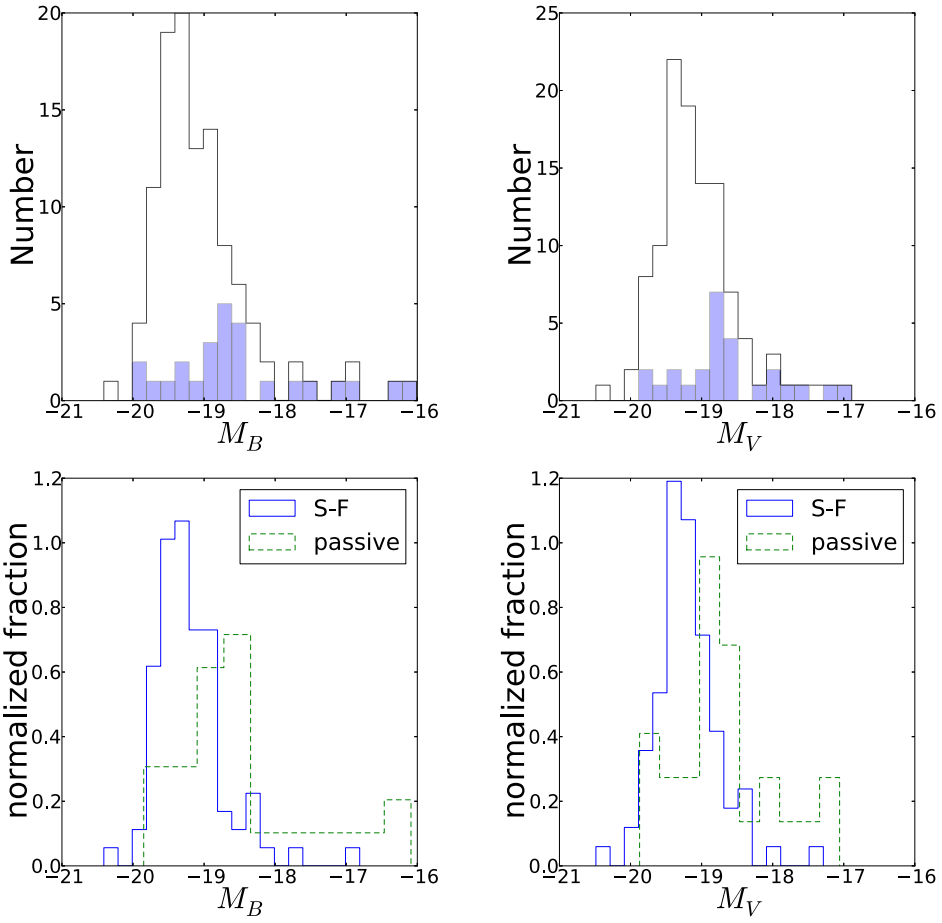

Figure 10. The above plots are the final M_B and M_V LD plots for the sample used in this paper. SNe Ia from passive galaxies with no known extinction have been re-added to this distribution to increase the sample size. Top: the left-hand plot is the full M_B LD, the right-hand plot is the full M_V LD. The overlaid blue histograms are the distributions of SNe from passive galaxies. Bottom: the left-hand plot is the full M_B LD separated by host galaxy type, and the right-hand plot is the full M_V distribution separated by host galaxy type.

We justify this step because it is reasonable to assume that SNe in passive galaxies have very little host extinction.[2] The new sample sizes comprise then 115 SNe, of which 89 are from S-F galaxies and 26 from passive galaxies. Fig. 10 is the final SN Ia LD. The mean absolute magnitudes of the full sample are $\bar{M}_B = -19.04 \pm 0.07$ mag and $\bar{M}_V = -19.07 \pm 0.06$ mag. Fig. 11 shows the final SNe Ia Δm_{15} distributions.

In Fig. 10 we plot the LD of SNe Ia, divided by host galaxy type. We can assume that at least three different populations of SNe Ia are present in these plots: a normal population of SNe Ia from S-F galaxies, which dominates the population of normal SNe, a normal population of SNe Ia from passive galaxies, and a subluminous population, which is dominated by SNe in passive galaxies. The numbers of subluminous SNe in S-F galaxies is too small to determine whether their population has different properties with respect to that in passive galaxies.

The shape of the LD depends strongly on host type. The LDs of SNe Ia in S-F galaxies have Gaussian shapes, with mean magnitudes $\bar{M}_B = -19.20 \pm 0.05$ mag and $\bar{M}_V = -19.19 \pm 0.05$ mag and standard deviations of 0.49 and 0.45 mag, respectively, see Table 6. In passive galaxies the SN Ia LD is much wider: the mean magnitudes are $\bar{M}_B = -18.48 \pm 0.19$ mag and $\bar{M}_V = -18.67 \pm 0.14$ mag, with standard deviations 0.49 and 0.98 mag, respectively.

To compare the distributions of 'normal' SNe Ia from the two different host galaxy types we must exclude subluminous SNe Ia. This is done by removing any SNe Ia with M_B, $M_V > -18.0$ mag. These values are obtained by visual inspection of the plots. It should be noted that the cut-off is applied in terms of absolute magnitude rather than decline rate, as fast declining SNe Ia can be both intrinsically bright and intrinsically dim (Fig. 9). The results are shown in Fig. 10.

When the subluminous population is removed, the distributions change. S-F galaxies have $\bar{M}_B = -19.24 \pm 0.04$ mag and $\bar{M}_V = -19.22 \pm 0.05$ mag, with median values $M_B = -19.27 \pm 0.05$ mag and $M_V = -19.25 \pm 0.06$ mag. For passive galaxies, $\bar{M}_B = -18.94 \pm 0.11$ mag, $\bar{M}_V = -18.94 \pm 0.10$ mag, with median values $M_B = -18.80 \pm 0.13$ mag and $M_V = -18.86 \pm 0.12$ mag.

The photometric distributions of 'normal' SNe Ia depends therefore on host galaxy types. The differences between the mean values of M_B and M_V are 0.30 ± 0.11 and 0.28 ± 0.11 mag, respectively, and are 0.47 ± 0.14 and 0.39 ± 0.13 mag in the median values. These two separate distributions lead us to the conclusion that within the 'normal' SNe Ia population, intrinsically dimmer SNe Ia are more common from older stellar populations, confirming previous results (e.g. Sullivan et al. 2006).

[2] The one exception is SN 1986G which was corrected for extinction of $E(B-V) = 0.65$ mag (Nugent et al. 1995). SNe 1986G is from an S0 galaxy, but sits in the dust lane in NGC 5128.

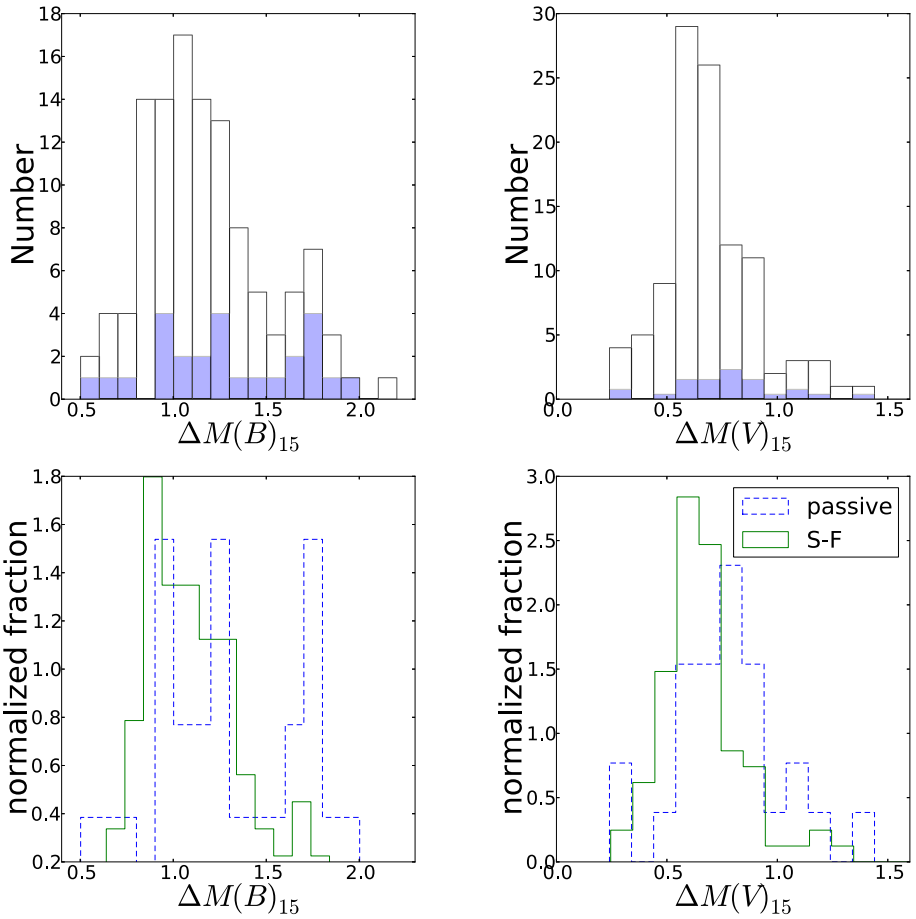

Figure 11. The final $\Delta M_{15}(B)$ and $\Delta M_{15}(V)$ LD plots for the sample used in this paper. SNe Ia from passive galaxies with no known extinction have been re-added to this distribution to increase the sample size. Top: the left-hand plot is the full $\Delta m_{15}(B)$ LD, the right-hand plot is the full $\Delta M_{15}(V)$ LD. The overlaid blue histograms are the distributions of SNe from passive galaxies. Bottom: the left-hand plot is the full $\Delta M_{15}(B)$ LD separated by host galaxy type, and the right-hand plot is the full $\Delta m_{15}(V)$ distribution separated by host galaxy type.

Table 6. Statistics of full LD.

	All	S-F	Passive
Amount of SNe	115	89	26
$\overline{M_B}$	-19.04 ± 0.07	-19.20 ± 0.05	-18.48 ± 0.19
σM_B	0.70	0.49	0.98
MedianM_B	-19.20 ± 0.08	-19.27 ± 0.07	-18.68 ± 0.24
$\overline{M_V}$	-19.07 ± 0.06	-19.19 ± 0.05	-18.67 ± 0.14
σM_V	0.57	0.45	0.72
MedianM_V	-19.16 ± 0.07	-19.24 ± 0.06	-18.78 ± 0.18
$\overline{M_B}^a$	-19.19 ± 0.04	-19.24 ± 0.04	-18.94 ± 0.11
σM_B	0.43	0.40	0.47
MedianM_B	-19.23 ± 0.05	-19.27 ± 0.05	-18.80 ± 0.13
$\overline{M_V}^b$	-19.16 ± 0.04	-19.22 ± 0.04	-18.94 ± 0.10
σM_V	0.43	0.41	0.46
MedianM_V	-19.19 ± 0.05	-19.25 ± 0.06	-18.86 ± 0.12

Notes. [a]$M_B < -18$ mag.
[b]$M_V < -18$ mag.

6 SNe Ia FROM YOUNG AND OLD STELLAR POPULATIONS

SNe Ia are thought to come from both young (<400 Myr) and old (>2.4 Gyr) stellar populations (Brandt, Tojeiro & Aubourg 2010). Traditionally, faster declining SNe Ia are thought to come from old stellar populations, and slower declining SNe Ia from young stellar systems. In Section 5 we have determined that there are at least three populations of SNe Ia: 'normal' SNe from S-F, 'normal' SNe from passive galaxies and subluminous SNe. As passive galaxies predominantly consist of old stars, we conclude that some of the 'normal' SNe Ia must originate from old stellar systems. On the other hand, S-F galaxies consist of both young and old stellar populations. Therefore they must contain SNe from both groups. In this section we attempt to quantify the fraction of SNe Ia from S-F galaxies which are produced from old stellar populations. From this the LD of SNe Ia from young stellar populations is produced.

We use the normalized LDs shown in Fig. 10 to determine the fraction of SNe Ia from young/old stellar populations. This is done by scaling the LD from passive galaxies and subtracting this distribution from SNe from S-F galaxies. It is known that SNe Ia with $M_B > -18$ mag are mostly from older stellar populations, so we examine only SNe Ia with $M_B < -18$ mag. Both LDs were divided into 20 bins with similar size (0.2 mag); so that the LDs can be scaled and subtract from one another. We scaled the passive LD to 10, 20, 30 and 40 per cent with respect to the S-F LD and subtract it. We are assuming that our sample of passive SNe Ia is a fair representation of the intrinsic sample, i.e. that SNe from passive environments in S-F galaxies have the same properties as

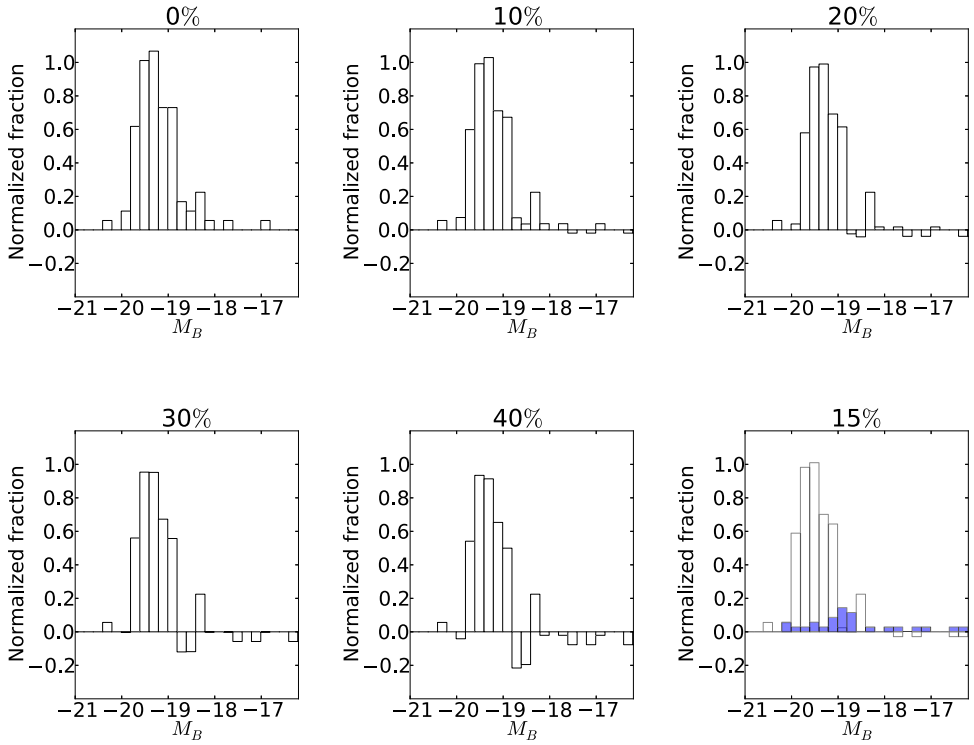

Figure 12. The *B*-band LD for SNe Ia from passive galaxies normalized, scaled and subtracted from the LD of SNe Ia from S-F galaxies. The factor by which the SNe Ia from passive galaxies has been normalized is presented on the top of each plot. The blue bars in the bottom right-hand panel are the LD of SNe Ia from passive galaxies scaled to 15 per cent of those from active galaxies.

SNe from passive galaxies. The scaled and subtracted S-F LDs are shown in Fig. 12, which shows that if the passive-like component exceeds 20 per cent of the total the subtraction is unrealistic as there are too many negative bins. Therefore, in the *B* band we select a value of (15 ± 10) per cent as the optimum scaling value to use in the LD subtractions, and suggest that this is the fraction of 'normal' SNe Ia in S-F galaxies which are from old stellar populations. The LD when a scaling factor of 15 per cent is used is shown in the bottom right-hand panel in Fig. 12, where we also show the 'passive' component. In the remaining plots of Fig. 12, we only show the result of the subtraction, i.e. the 'young' component. The LD of SNe Ia from young stellar systems is narrower than that of the whole sample. This effect is seen in both the *B* and *V* bands. Fig. 13 shows the *V*-band scaled and subtracted LDs. The *V*-band results also suggest that (15 ± 10) per cent of 'normal' SNe Ia from S-F galaxies are from old stellar populations. The bottom right-hand panel in Fig. 13 presents the *V*-band LD when a scaling factor of 15 per cent is chosen. The blue bars overlaid in this plot show the LD of SNe Ia from passive galaxies scaled to 15 per cent. Therefore we conclude that there are photometrically four populations of SNe Ia: 'normal' ones from S-F galaxies that come from young stellar systems, 'normal' SNe Ia from passive galaxies that come from an old population, 'normal' SNe Ia from S-F galaxies that come from an old population and subluminous SNe that are thought to come from old stellar systems.

If we assume that our sample is complete, and use $M_B < -18$ mag as the cut-off between subluminous and normal SNe Ia, the frequency of SNe Ia in our sample can be quantified. Out of the 115 SNe Ia in Fig. 10, eight (7 per cent) are subluminous. This leaves 107 SNe Ia, of which 20 are 'normal' SNe Ia from passive galaxies (from an old population), and 16 are 'normal' SNe Ia from S-F galaxies and come from an old population. Therefore, 32 (28 per cent) of all SNe Ia are normal and come from an old population. Which means, 75 (65 per cent) of SNe Ia are normal and come from a young stellar population.

7 DISCUSSION

The aim of this work was to explore the diversity of SN Ia the LCs. Therefore, we built LDs using as few prior assumptions as possible. We have not relied on any empirical LC fitting method, and used distances to the SNe derived from independent methods. We chose to use mean values of $\Delta M_{15}(B/V)$ and $M_{B/V}$ for our analysis because this is a good way to highlight outliers, which make up a small fraction of the overall population. The analysis is presented both before and after applying a corrected for host galaxy extinction. Deriving the host galaxy extinction of SNe Ia is a difficult task as it requires resolving the degeneracy between colour and extinction. Although the method used for calculating the host galaxy extinction can resolve the colour–extinction degeneracy, it does remove the intrinsically unusual SNe, as there are not enough unreddened spectral matches. Only a subset of the SNe can be corrected for extinction, and some peculiar SNe may not pass this cut. Therefore, the true diversity of SNe Ia may be underrepresented in the corrected sample.

Before correction for host galaxy extinction, our sample includes 165 SNe Ia, 134 of which are from S-F galaxies, 26 from passive galaxies and five from host galaxies whose type could not be determined. The average M_B and M_V for the sample are −18.58 ±0.07 and −18.72 ±0.05 mag, respectively. The average $\Delta m_{15}(B)$ and $\Delta m_{15}(V)$ values for the sample are 1.14 ± 0.03 and 0.68 ± 0.01 mag.

We find a bimodal distribution in $\Delta m_{15}(B)$ (Fig. 3), with a lack of transitional SNe. Transitional SNe such as 1986G, 2003hv and iPTF13ebh all have unique properties, and can hold information

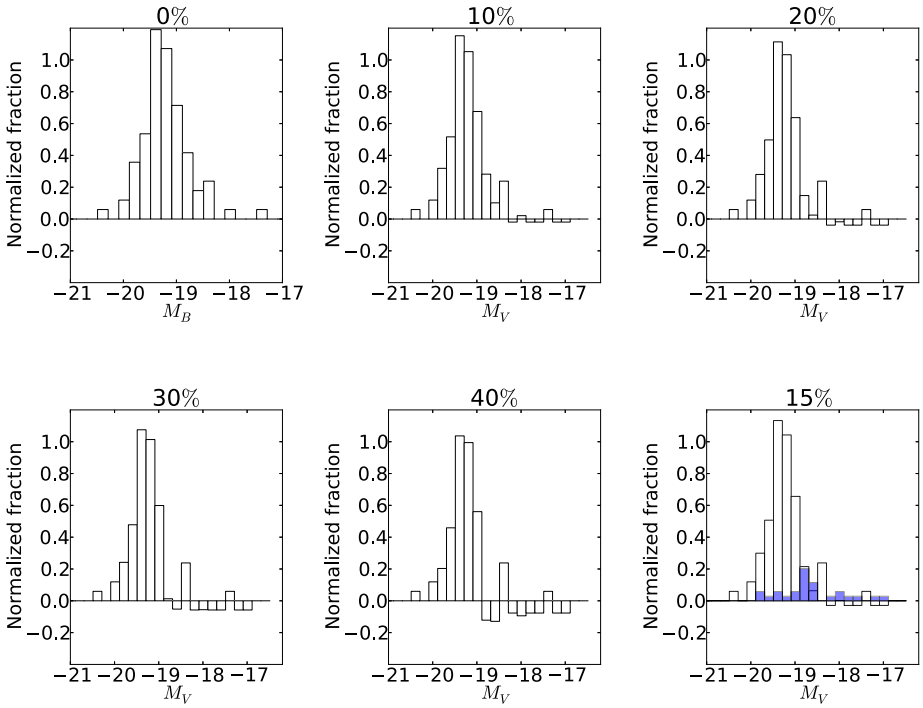

Figure 13. The *V*-band LD for SNe Ia from passive galaxies normalized, scaled and subtracted from the LD of SNe Ia from S-F galaxies. The factor by which the SNe Ia from passive galaxies has been normalized is presented on the top of each plot. The blue bars in the bottom right-hand panel are the LD of SNe Ia from passive galaxies scaled to 15 per cent of those from active galaxies.

about potential differences between progenitor channels of subluminous and normal SNe Ia. If it is not a selection effect, the lack of transitional SNe could suggest that SNe Ia may come from multiple populations, with different LC properties, which only cross in $\Delta m_{15}(B)$ at their extremes.

Correcting the data for host galaxy extinction reduces the sample size to 109 SNe Ia, 89 of which are from S-F galaxies, 16 from passive galaxies and five from host galaxies whose type could not be determined. The smaller sample is comparable to the larger sample in most relevant parameters. SNe Ia from S-F galaxies suffer from much larger host extinction than those from passive galaxies: 67 per cent of the SNe Ia from S-F galaxies are affected by detectable host galaxy extinction, whose the average value is $E(B-V) = 0.130 \pm 0.023$ mag. In contrast, only 43 per cent of the SNe Ia from passive galaxies are affected by detectable extinction, with average $E(B-V) = 0.04 \pm 0.013$ mag. When corrected for host galaxy extinction, the mean $\bar{M}_B = -19.09 \pm 0.06$ mag and $\bar{M}_V = -19.10 \pm 0.05$ mag. In the *B*-band SNe from passive galaxies were found to be 0.63 ± 0.25 mag less luminous on average than SNe in S-F galaxies. The same is true in the *V* band, where the difference is 0.48 ± 0.19 mag.

The WLR is one of the underlying foundations in SN Ia cosmology. It is driven by Ni mass, opacity and ejecta mass. We find a strong correlation between $\Delta m_{15}(B)$ and absolute magnitude for normal SNe when only SNe with have a small observed colour term are selected. The WLR in our study is similar to those of Phillips (1993) and Phillips et al. (1999). However, after correcting for host galaxy extinction the spread of properties increases, as shown in Fig. 9. Furthermore, correcting for reddening leads to the removal of some of the more unusual SNe Ia, and so the true parameter space SNe Ia can fill in the WLR diagram is probably even larger.

K–S tests were run on the sample after correction for extinction. The probability that M_B values for SNe Ia from passive and S-F galaxies come from the same parent distribution was found to be <0.1 per cent. In the case of M_V the probability is <0.4 per cent. The likelihood that the $\Delta m_{15}(B)$ samples come from the same parent distributions is $\simeq$12 per cent.

SNe Ia in passive galaxies for which the extinction could not be derived were reintroduced to the extinction-corrected sample. As only 43 per cent of the SNe Ia from passive galaxies were affected by detectable host galaxy extinction, and this average extinction was very small, we assumed that the reintroduced sample has negligible host extinction. When the final LD is separated by host galaxy type, it is found that there are three main populations of SNe Ia: 'normal' SNe Ia in S-F galaxies, 'normal' SNe Ia in passive galaxies and subluminous SNe Ia. Normal SNe Ia in S-F galaxies were found to have a median $M_B = -19.27 \pm 0.05$ mag and $M_V = -19.25 \pm 0.06$ mag. Normal ($M_B < -18$) SNe Ia in passive galaxies have median $M_B = -18.80 \pm 0.13$ mag and $M_V = -18.86 \pm 0.12$ mag. The difference hints at differences in properties of normal SNe Ia depending on host galaxy type, as shown in Fig. 10. SNe Ia in S-F galaxies appear to be a much more uniform sample: their distribution is similar to a Gaussian, whereas SNe Ia in passive galaxies appear to be far more diverse.

In the final section of the analysis we normalize the LDs for SNe Ia from passive and S-F galaxies. In order to quantify the fraction of 'normal' SNe Ia which come from old stellar systems in S-F galaxies we scaled the LD of SNe Ia from passive galaxies to represent different fractions of the full S-F LD and subtracted it from the full S-F LD. We find that (15 ± 10) per cent of 'normal' SNe Ia from S-F galaxies are likely to come from old stellar systems.

In order fully to explore the range in parameter space that SNe Ia can fill one would need to obtain a large sample LF, in both redshift and volume, which is out of the scope of our study. Yasuda & Fukugita (2010) produced a LF, however, they removed any peculiar SNe Ia and did not break the colour-reddening degeneracy.

Li et al. (2011) produced a volume-limited LF, but did not correct for host galaxy extinction.

As transitional objects appear to be rare, a large sample survey would have to operate continuously for many years to produce a comprehensive LF of SNe Ia. In the years of the Large Synoptic Survey Telescope (LSST) and large high cadence surveys, along with robotic telescopes on multiple sites [Las Cumbres Observatory Global Telescope (LCOGT)], this will be possible. We will then be able to know the variance of SNe Ia and place tighter constraints on the progenitor systems.

8 CONCLUSIONS

This paper takes a different approach to SN Ia LC analysis. We made as few assumptions as possible about the SNe, so two SNe Ia with a similar LC shape can have different properties. This way it is possible to explore the diversity of SNe Ia. We studied SNe Ia by first independently obtaining the distance to each one then calculating its properties, M_B, $\Delta m_{15}(B)$, M_V and $\Delta m_{15}(V)$. This allowed us to see the parameter space that SNe Ia can fill.

We confirm previous results that SNe in passive galaxies tend to decline more rapidly, with an average $\Delta m_{15}(B) = 1.29 \pm 0.08$ mag, compared to $\Delta m_{15}(B) = 1.11 \pm 0.03$ mag for SNe in S-F galaxies. This is partly due to the presence of subluminous SNe Ia, which are mostly found in older stellar populations. Our method confirms that SNe with small observed $(B - V)_{B_{\max}} < 0.01$ mag follow the WLR, with some scatter. However, when a larger sample of SNe are corrected for host galaxy extinction the scatter in the WLR increases. We find that the range in M_B of normal SNe Ia in the WLR is $\sim$1.5 mag. This suggests that (intrinsically) SNe Ia can fill a large parameter space on the WLR. The distribution in $\Delta m_{15}(B)$ was found to be bimodal, with a lack of transitional SNe. More data from transitional SNe can hold the key to fully understanding the explosion mechanisms of the faint end of the 'normal' SNe on the WLR.

We find evidence for differences in parameters for SNe Ia from different host galaxies. SNe Ia in passive galaxies are more likely to be peculiar than those in S-F galaxies. These peculiarities could be central in the debate on different progenitor systems or populations. We found that there are three main populations of SNe Ia: normal SNe Ia in S-F galaxies, normal SNe Ia in passive galaxies and subluminous SNe Ia. Normal ($M_V < -18$ mag) SNe from passive galaxies have a median $M_V = -18.86 \pm 0.12$ mag, while those from S-F galaxies have a median $M_V = -19.25 \pm 0.06$ mag. Finally, we find that (15 ± 10) per cent of 'normal' SNe Ia from S-F galaxies are likely to come from old stellar systems.

SNe Ia are, although 'standardizable', not an extremely homogeneous group of objects. There are unusual events which could possibly result from multiple progenitor scenarios. We have confirmed previous results that subluminous SNe favour passive galaxies, and have raised questions about the nature of 'normal' SNe Ia from passive galaxies. The key to examining these differences further could be through finding a convincing method to calculate host galaxy extinction on unusual SNe Ia, and with this it will be possible to put tighter constraints on the parameter space SNe Ia can fill.

ACKNOWLEDGEMENTS

The authors would like to thank Mark Sullivan and Chris Usher for advice on how to treat the data. The authors would also like to thank the anonymous referee for helpful comments and advice. The authors would like to thank the SNDB team for releasing their data to the public. This research has made use of the NASA/IPAC Extragalactic Database (NED) which is operated by the Jet Propulsion Laboratory, California Institute of Technology, under contract with the National Aeronautics and Space Administration. This research has made use of the CfA Supernova Archive, which is funded in part by the National Science Foundation through grant AST 0907903.

REFERENCES

Altavilla G. et al., 2007, A&A, 475, 585
Anupama G. C., Sahu D. K., Jose J., 2005, A&A, 429, 667
Ashall C., Mazzali P., Bersier D., Hachinger S., Phillips M., Percival S., James P., Maguire K., 2014, MNRAS, 445, 4427
Brandt T. D., Tojeiro R., Aubourg É., 2010, AJ, 140, 804
Burns C. R., Stritzinger M., Phillips M. M., Hsiao E. Y., 2014, ApJ, 789, 32
Cardelli J. A., Clayton G. C., Mathis J. S., 1989, ApJ, 345, 245
Childress M. et al., 2013, ApJ, 770, 107
Chotard N., Gangler E., Aldering G., 2011, A&A, 529, L4
Conley A. et al., 2008, ApJ, 681, 482
Deng J. et al., 2004, ApJ, 605, L37
Dilday B. et al., 2012, Science, 337, 942
Dong S., Katz B., Kushnir D., Prieto J. L., 2015, MNRAS, 454, L61
Elias-Rosa N. et al., 2006, MNRAS, 369, 1880
Fisher A., Branch D., Hatano K., Baron E., 1999, MNRAS, 304, 67
Folatelli G., Phillips M. M., Burns C. R., 2010, AJ, 139, 120
Ganeshalingam M., Li W., Filippenko A. V., 2010, ApJS, 190, 418
Guy J. et al., 2007, A&A, 466, 11
Guy J., Sullivan M., Conley A., Regnault N., 2010, A&A, 523, A7
Hachinger S., Mazzali P. A., Benetti S., 2006, MNRAS, 370, 299
Hachinger S., Mazzali P. A., Taubenberger S., Fink M., Pakmor R., Hillebrandt W., Seitenzahl I. R., 2012, MNRAS, 427, 2057
Hamuy M., Phillips M. M., Maza J., Suntzeff N. B., Schommer R. A., Aviles R., 1995, AJ, 109, 1
Hamuy M., Phillips M. M., Suntzeff N. B., Schommer R. A., Maza J., Antezan A. R., 1996, AJ, 112, 2408
Hamuy M. et al., 2003, Nature, 424, 651
Hicken M., Challis P., Jha S., Kirshner R. P., Matheson T., Modjaz M., Rest A., 2009, ApJ, 700, 331
Hicken M. et al., 2012, ApJS, 200, 12
Hillebrandt W., Niemeyer J. C., 2000, ARA&A, 38, 191
Höflich P., Gerardy C. L., Fesen R. A., Sakai S., 2002, ApJ, 568, 791
Howell D. A., 2001, ApJ, 554, L193
Howell D. A. et al., 2006, Nature, 443, 308
Hsiao E. Y., Burns C. R., Contreras C., 2015, A&A, 578, A9
Iben I., Jr, Tutukov A. V., 1984, ApJS, 54, 335
Jha S., Riess A. G., Kirshner R. P., 2007, ApJ, 659, 122
Katz B., Dong S., 2012, preprint (arXiv:1211.4584)
Kessler R., Becker A. C., Cinabro D., 2009, ApJS, 185, 32
Krisciunas K. et al., 2003, AJ, 125, 166
Krisciunas K., Phillips M. M., Suntzeff N. B., Persson S. E., Hamuy M., Antezana R., 2004a, AJ, 127, 1664
Krisciunas K., Phillips M. M., Suntzeff N. B., 2004b, ApJ, 602, L81
Kromer M. et al., 2015, MNRAS, 450, 3045
Kushnir D., Katz B., Dong S., Livne E., Fernández R., 2013, ApJ, 778, L37
Leloudas G., Stritzinger M. D., Sollerman J., 2009, A&A, 505, 265
Lentz E. J., Baron E., Branch D., Hauschildt P. H., Nugent P. E., 2000, ApJ, 530, 966
Li W. et al., 2003, PASP, 115, 453
Li W. et al., 2011, MNRAS, 412, 1441
Lira P., Suntzeff N. B., Phillips M. M., Hamuy M., Maza J., Schommer R. A., Smith R. C., Wells L. A., 1998, AJ, 115, 234
Maguire K., Sullivan M., Thomas R. C., Nugent P., Howell D. A., Gal-Yam A., Arcavi I., Ben-Ami S., 2011, MNRAS, 418, 747
Maguire K. et al., 2014, MNRAS, 444, 3258
Mandel K. S., Foley R. J., Kirshner R. P., 2014, ApJ, 797, 75
Mazzali P. A., Hachinger S., 2012, MNRAS, 424, 2926

Mazzali P. A., Danziger I. J., Turatto M., 1995, A&A, 297, 509
Mazzali P. A., Röpke F. K., Benetti S., Hillebrandt W., 2007, Science, 315, 825
Mazzali P. A., Maurer I., Stritzinger M., Taubenberger S., Benetti S., Hachinger S., 2011, MNRAS, 416, 881
Mazzali P. A. et al., 2014, MNRAS, 439, 1959
Mould J. R., Huchra J. P., Freedman W. L., Kennicutt R. C., Jr, Ferrarese L., Ford H. C., 2000, ApJ, 529, 786
Muratov A. L., Gnedin O. Y., 2010, ApJ, 718, 1266
Nomoto K., Iwamoto K., Kishimoto N., 1997, Science, 276, 1378
Nugent P., Phillips M., Baron E., Branch D., Hauschildt P., 1995, ApJ, 455, L147
Oke J. B., Sandage A., 1968, ApJ, 154, 21
Pan Y.-C., Sullivan M., Maguire K., Gal-Yam A., Hook I. M., Howell D. A., Nugent P. E., Mazzali P. A., 2015, MNRAS, 446, 354
Pastorello A., Mazzali P. A., Pignata G., Benetti S., Cappellaro E., Filippenko A. V., Li W., 2007, MNRAS, 377, 1531
Phillips M. M., 1993, ApJ, 413, L105
Phillips M. M. et al., 1987, PASP, 99, 592
Phillips M. M., Lira P., Suntzeff N. B., Schommer R. A., Hamuy M., Maza J., 1999, AJ, 118, 1766
Rest A., Scolnic D., Foley R. J., 2014, ApJ, 795, 44
Riess A. G., Press W. H., Kirshner R. P., 1996, ApJ, 473, 88
Riess A. G. et al., 1998, AJ, 116, 1009
Riess A. G., Kirshner R. P., Schmidt B. P., Jha S., Challis P., Garnavich P. M., Esin A., 1999, AJ, 117, 707
Riess A. G., Li W., Stetson P. B., Filippenko A. V., Greenhill L., Jha S., 2005, Am. Astron. Soc. Meeting Abstr., 180.10
Rigault M. et al., 2013, A&A, 560, A66
Rosswog S., Kasen D., Guillochon J., Ramirez-Ruiz E., 2009, ApJ, 705, L128
Sahu D. K. et al., 2008, ApJ, 680, 580
Sasdelli M., Mazzali P. A., Pian E., Nomoto K., Hachinger S., Cappellaro E., Benetti S., 2014, MNRAS, 445, 711
Sasdelli M., Ishida E. E. O., Hillebrandt W., Ashall C., Mazzali P. A., Prentice S., 2016, MNRAS, preprint (arXiv:e-prints)
Sauer D. N. et al., 2008, MNRAS, 391, 1605
Schlafly E. F., Finkbeiner D. P., 2011, ApJ, 737, 103
Silverman J. M. et al., 2013, ApJS, 207, 3
Sullivan M., Le Borgne D., Pritchet C. J., Hodsman A., Neill J. D., Howell D. A., Carlberg R. G., 2006, ApJ, 648, 868
Sullivan M. et al., 2010, MNRAS, 406, 782
Taubenberger S., Hachinger S., Pignata G., Mazzali P. A., Contreras C., Valenti S., 2008, MNRAS, 385, 75
Tripp R., 1998, A&A, 331, 815
Valentini G., Di Carlo E., Massi F., Dolci M., Arkharov A. A., Larionov V. M., Pastorello A., 2003, ApJ, 595, 779
Wang X., Wang L., Filippenko A. V., Zhang T., Zhao X., 2013, Science, 340, 170
Yamanaka M. et al., 2009, ApJ, 707, L118
Yamanaka M. et al., 2014, ApJ, 782, L35
Yasuda N., Fukugita M., 2010, AJ, 139, 39

APPENDIX A

Table A1 presents the references of the SNe which have come from individual papers.

Table A1. The reference of the 11 SNe Ia mentioned in Table 1.

SNe name	Reference
SN 1986G	Phillips et al. (1987)
SN 1990N	Lira et al. (1998)
SN 1991bg	Krisciunas, Phillips & Suntzeff (2004b)
SN 1991T	Krisciunas et al. (2004b)
SN 1998aq	Riess et al. (2005)
SN 2000ca	Krisciunas et al. (2004a)
SN 2000E	Valentini et al. (2003)
SN 2001bt	Krisciunas et al. (2004b)
SN 2001cz	Krisciunas et al. (2004b)
SN 2001el	Krisciunas et al. (2003)
SN 2003du	Anupama, Sahu & Jose (2005)

APPENDIX B: QUALITY OF LC SPINE FIT

In this section we quantify the quality of our spline LC fits. In Fig. B1 we have plotted, in the *B* band, the residuals between the SN data and fitted LC for 46 randomly selected SN from the sample. The residuals in this plot are less than 0.05 mag for each SN. These are significantly smaller than the errors, which were taken as the errors on the photometric data. We can produce such small residuals as we only fit the LC until 20 d past maximum, and only SN with very good temporal coverage is selected. Fig. B2 shows the same residuals using the *V* band, the residuals for these bands are also less than 0.05 mag. The residuals in these plots are constant as a function of time, therefore, we have no systematic residuals with phase. We have not plotted the residuals for the errors as a MC approach has been used.

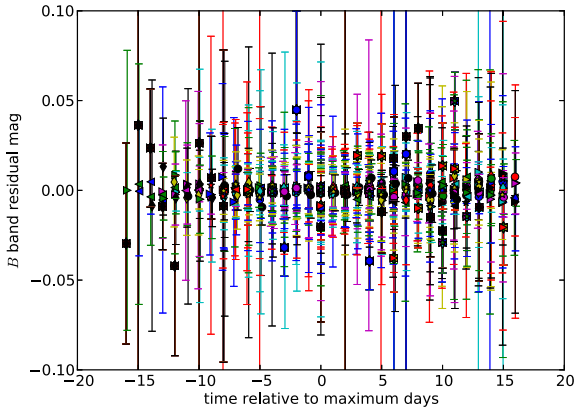

Figure B1. The *B*-band residuals from the SN photometry and LC spline fit, as a function on time. Data from 46 randomly selected SNe are used.

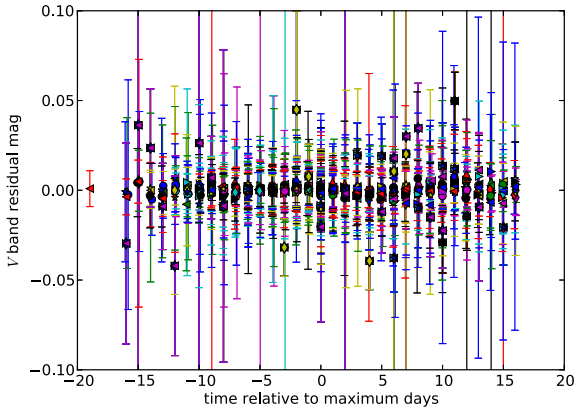

Figure B2. The *V*-band residuals from the SN photometry and LC spline fit, as a function on time. Data from 46 randomly selected SNe are used.

This paper has been typeset from a TEX/LATEX file prepared by the author.